Heat Flux Instrumentation for Hyflite Thermal Protection System

NLPN 93-428
NAG-1-1538

Final Report

Principal Investigator: T. E. Diller
Mechanical Engineering Dept.
Virginia Tech
Blacksburg, VA 24061-0238

Funding Period: Aug. 13, 1993 - Jan. 13, 1994

NASA Technical Officer: Dr. G. Burton Northam
FLDMD, MS 170
NASA Langley Research Center
Hampton, VA 23681-0001

Summary of Results

Vatell Corp. was successful in performing all of the necessary tasks associated with this contract. Using Thermal Protection Tile core samples supplied by NASA, the surface characteristics of the FRCI, TUFI, and RCG coatings were evaluated. Based on these results, appropriate methods of surface preparation were determined and tested for the required sputtering processes. Sample sensors were fabricated on the RCG coating and adhesion was acceptable. Based on these encouraging results, complete Heat Flux Microsensors were fabricated on the RCG coating. The issue of lead attachment was addressed with the annealing and welding methods developed at NASA Lewis. Parallel gap welding appears to be the best method of lead attachment with prior heat treatment of the sputtered pads. Sample Heat Flux Microsensors were delivered to Herb Will at NASA Lewis for testing in the NASA Ames arc jet facility. Testing is still continuing at this writing. Details of the project are contained in the two attached reports from Vatell Corp.

One additional item of interest is contained in the attached AIAA paper, which gives details of the transient response of a Heat Flux Microsensor in a shock tube facility at Virginia Tech. The response of the heat flux sensor was measured to be faster than 10 μs.

Application of Heat Flux Microsensors to HYFLITE Thermal Protection Tiles

PROGRESS REPORT #1 - VPI Contract FP-4578-426350

Period of Report - 9/8/93 through 11/15/93

VATELL CORPORATION
P.O. Box 66
Christiansburg, VA 24073

SUMMARY

Vatell received two lots of Thermal Protection Tile (TPT) core samples prepared by NASA Ames. The first lot consisted of nine core samples nominally 1.0" diameter and 1.0" long. Three of these core samples had been coated with FRCI 12, three with FRCI 20, and three with FRCI 12 and RCG. The second lot of core samples contained an additional twelve FRCI 12 core samples with the same dimensions. The second lot is being held in reserve until studies with the first lot are completed. Vatell also received documentation and technical papers describing the TPT material and the FRCI, TUFI, and RCG coatings.

We concluded from preliminary experiments that the surface of the RCG coated core samples is more suitable for application of Heat Flux Microsensors than that of the FRCI coated core samples. A complete Heat Flux Microsensor was sputtered onto a polished RCG coated core sample (Figure 1) with moderate success. We have made adjustments to the fabrication process to correct the partial loss of adhesion which occurred in this experiment.

SURFACE EVALUATION

Surface quality is the most reliable predictor of success in the deposition of Heat Flux Microsensors. Assuming that the chosen conductor and insulator materials are chemically compatible and thermally matched to the surface material, roughness is the principal limiting factor in achieving adhesion. If the surface roughness is equal to or greater than the sputtered film thickness, the film will be more easily fragmented by thermal stresses. Roughness interferes with continuity of the thin film. An excessively rough surface is also detrimental to the masking process because the masks are physically held away from the surface. Some material is sputtered under the edges of the mask, and pattern sharpness is degraded.

The first priority in this project was to evaluate the surfaces of the different coatings on the TPT to find out if any of them could be processed using Vatell's standard techniques for fabrication of Heat Flux Microsensors. The FRCI 12 core samples are fully coated but still quite fibrous. The FRCI coating soaks into the tile material but has little effect on surface quality. The FRCI 20 core sample is also fully coated and has similar surface quality to the FRCI 12 but appears smoother under a microscope. The FRCI 12 with the RCG coating is glassy in appearance, but has a rippled surface. This surface appears to be the densest and most suitable for deposition of sputtered films.

We used a stylus profilometer to quantify the surface roughness of the different coatings. We could not perform these measurements with an optical profilometer without coating the surface with a reflective material. The optical profilometer is generally limited to measurements of surfaces with an average roughness better

than 1 micron. The stylus profilometer gave the following results for one of each of the different types of core samples:

Core sample Material	Average Surface Roughness (RA)
FRCI 12 (#541)	8.8 - 10 micron
FRCI 20 (#538)	8.1 - 9.0 micron
FRCI 12 - RCG (#3358)	3.0 - 3.2 micron

The stylus scans on the core samples without RCG coating revealed a large number of sharp peaks and steep valleys across the surface (Figures 2A - 2C). Without additional coatings or processing, a thin film will not maintain continuity on this type of surface. The RCG coating could possibly be used without any finishing, but for our first attempts we decided to polish the surface.

OUTGASSING TESTS

The next step before doing any surface processing was to check an RCG coated tile core sample for outgassing under vacuum. These initial tests were performed with the TPT mounted in a fixture designed for 0.25" x 1.0" disks. With this type of fixture the part is heated on the uncoated end by quartz lamps. Since the TPT is a very poor conductor of heat, it was difficult to determine the surface temperature with any accuracy. We measured (1) initial outgassing of the TPT under vacuum, (2) while bombarding its surface with an ion beam, and (3) while heating it in the vacuum.

We first measured the gases in the empty vacuum chamber with a residual gas analyzer, saving the scan from 1 AMU to 40 AMU. This scan was then compared with the three tests listed above. When the TPT was loaded into the chamber a small amount of water vapor and low levels of nitrogen and oxygen were introduced. The amounts were measured by subtracting the saved scan from this new scan. We took a scan on the same core sample while bombarding the surface with an ion beam for 10 minutes. The levels of water vapor increased. When the TPT was heated to an elevated temperature there was a substantial increase in the outgassing of water vapor as well as a small increase in nitrogen and oxygen. Unfortunately, a defect in the residual gas analyzer's software prevented us from saving the results of the differential scans.

We concluded that the tiles will require several hours of heating prior to deposition to allow water vapor outgassing to decrease to acceptable levels.

SPUTTERING FIXTURES

We have found in the past that accurate control of the substrate surface temperature is required during sputtering for good adhesion of multiple layers. Recognizing that we could not rely on conduction of heat through the core, we decided to design a sputtering fixture with a means for distributing heat to the front surface of the core sample. The fixture, shown in Figure 3, consists of a hollow cylinder attached to a flat plate. The cylinder is made from aluminum, black anodized to enhance its emissivity. The core sample is inserted in the cylinder and captured by two set screws near the bottom of the cylinder. The set screws form indentations in the TPT which prevent both rotation and axial movement of the core sample. The mask frame is fitted over three studs, clamping the mask against the substrate for deposition. The baseplate of the fixture is heated by quartz lamps. Heat is conducted to the cylinder and along it to the mask frame. The inner surface of the cylinder radiates to the sides of the TPT and the mask frame heats the front surface of the TPT by conduction. To be certain that the surface reaches the set temperature, we allow the part to heat for two hours. Although this method of heating is slow and inefficient, it works. A better method might be to have radiant lamps directed at the face of the tile. However, the lamps would have to be protected from sputtering by a movable shutter. This would require extensive modifications to the vacuum system, which we will only perform if the initial test results indicate that they are needed.

SURFACE PREPARATION

The surface quality of the core samples as received at Vatell was judged not to be good enough for direct application of a Heat Flux Microsensor. We decided to prepare the surfaces by polishing. FRCI 12 and FRCI 12 RCG core samples were polished using water-based diamond slurries. The core samples were hand-held in contact with polishing pads, each carrying a different slurry, progressing downward in size from 15 microns to 3 microns. Only the faces of the core samples were rinsed before progressing to the next smaller particle size. We found it difficult to fully clean the core samples because of their porosity. A great deal of the diamond slurry was absorbed into the sides of the TPT. By the end of the polishing process we realized that the core sample had absorbed as much water from polishing and surface rinsing as it might have if we had cleaned it ultrasonically from the start.

The RCG coated core sample required a few hours of polishing with 15 micron to achieve a flat smooth surface. Less time was required on the 6 micron and 3 micron levels except when a piece of RCG chipped off the edges and was carried around to scratch the core sample surface. Each time this occurred it was necessary to start over with the 15 micron slurry. The end result of this process was a very smooth and shiny surface (Figure 2D).

We also polished the FRCI 12 without the RCG, using 15 micron slurry, for many hours. As material was removed on the surface a similar surface was revealed. The porosity and coarse fibers did not lend themselves to being polished or to achieving a flat surface. We could not improve the surface (Figure 2E) even by using a 15 micron solid grinding wheel.

We performed a stylus scan to measure the level of improvement of surface preparation. The results were as follow:

Core Sample Material	Average Surface Roughness (RA)
FRCI 12 (#541)	> 10.0 micron
FRCI 12 - RCG (#3358)	0.068 - 0.09 micron

We experienced many problems in handling the RCG coated TPT core samples during polishing. Attempting to reduce the time required to achieve a flat surface, we chose a 30 micron slurry. After the edge chipping experiences with the RCG coated core samples we decided to design a holding fixture for polishing. This gave the polishing operator a larger surface to handle, and protected the core sample from damage.

The holding fixture (Figure 4) is an aluminum cylinder which holds the face of the core sample flush at one end. The cylinder is made in two halves so when it is clamped around the core sample it applies a uniform pressure. We added thin strips of rubber inside the cylinder to capture the part rigidly without points of pressure. We also hoped that the rubber strips around the circumference close to the face would eliminate water absorption by the core sample but this was found to be incorrect. Slurry seeped its way into the fixture and then leaked out during subsequent polishing, contaminating the finer slurry.

When we mounted an RCG coated core sample in the fixture, we found that its face could not be made flush with the end. The face of the core sample was not perpendicular to its side. The mismatch was great enough so that if the core sample were ground flush with the end of the fixture the RCG material would be completely removed. We were able to use the fixture but the core sample had to protrude from the end to compensate for its lack of perpendicularity.

Using the new fixture we prepared two more RCG coated core samples. The initial time to flatten the surface was reduced using the 30 micron slurry. The polishing process was also improved by using new polishing pads for each core sample to eliminate carry-over of abrasives and chips. While there was still some chipping around the circumference of the coating, the RCG polished to a very good finish with the 3 micron slurry. We used the ultrasonic bath between each step to reduce abrasive carry-over. The core samples were dried in an oven for 4 - 6 hours prior to taking them into the cleanroom.

FABRICATION OF HEAT FLUX MICROSENSOR

Herb Will of NASA Lewis informed Vatell that he had succeeded in getting adhesion of a platinum - platinum/10% rhodium thermocouple on an RCG coated tile. To conserve experiment time, we decided to attempt application of a complete Heat Flux Microsensor to the RCG surface.

We thoroughly cleaned the surface of the polished RCG core sample under vacuum, using an energetic ion shower. The ion shower was applied until there was a noticeable change in the surface in the region of fabrication. Then we deposited an aluminum oxide layer on the surface to help seal the RCG layer. The 7 remaining layers of silicon monoxide, aluminum oxide, platinum and platinum/10% rhodium were deposited in succession to form the sensor. Following the usual procedure we aligned each of the stencil masks under a microscope. Adhesion appeared to be very satisfactory until the top layer of aluminum oxide was deposited. This layer is applied to seal the sensor against oxygen and mechanically protect it. After this deposition, adhesion was lost at several sites on the pattern. In all these sites there were multiple layers of ceramic and metal. The stress imposed by shrinkage of the ceramic coating was sufficient to overcome the adhesion of the metal layers. The failure was largely a function of adhesion at the interface between successive layers.

A Scotch tape pull test revealed that there was a substantial adhesion loss in the metalization layers at the interface with the deposited aluminum oxide. This was probably a result of surface contamination or incorrect stoichiometry of the aluminum oxide. The adhesion loss was only partial; a promising sign. Documentary photographs were taken of the core sample prior to the tape test. These have been copied and sent to Herb Will at NASA Lewis and Fred Kern at NASA Langley.

We have started fabrication on the second RCG coated core sample. This core sample was given a long pre-clean with the ion source before application of the first mask. The part was subjected to a second ion shower with the mask in place for a short period immediately prior to thin film deposition. For each subsequent layer there will be a brief preclean by the ion beam with the mask in place. We hope that this additional process step will promote adhesion between successive layers by removing small scale contaminants. These ion showers will be performed at an elevated temperature to enhance contaminant removal.

The base layer of aluminum oxide was not applied on this core sample. It will be photographed prior to deposition of the top layer of aluminum oxide if adhesion is satisfactory. The core sample will then be annealed from 1000°C at -0.3°C/min. in an effort to relieve any residual stresses at the film interfaces. An argon atmosphere may be required to prevent oxidation of the rhodium. Following the anneal, the protective layer will be deposited.

PROJECTED PLANS

Results of the next sensor fabrication will be evaluated. If there is an adhesion failure, the interface at which it occurred will be identified. We may need to substitute another material for one or more of the thin film components. Longer ion shower treatments may be required between layers. Simple layered film experiments will be performed on the first TPT core sample to check interface adhesion. An SEM analysis with EDAX will be performed on those layers whose interface lost adhesion to check the stoichiometry and determine if there are any contaminants present.

Tests will begin on the TUFI coated core samples which have just been received. These will include surface analysis, preparation, film coatings, and sputtered layer adhesion and continuity tests. The objective is to have a complete Heat Flux Microsensor on a TUFI coated TPT survive Vortek tests by the end of the year.

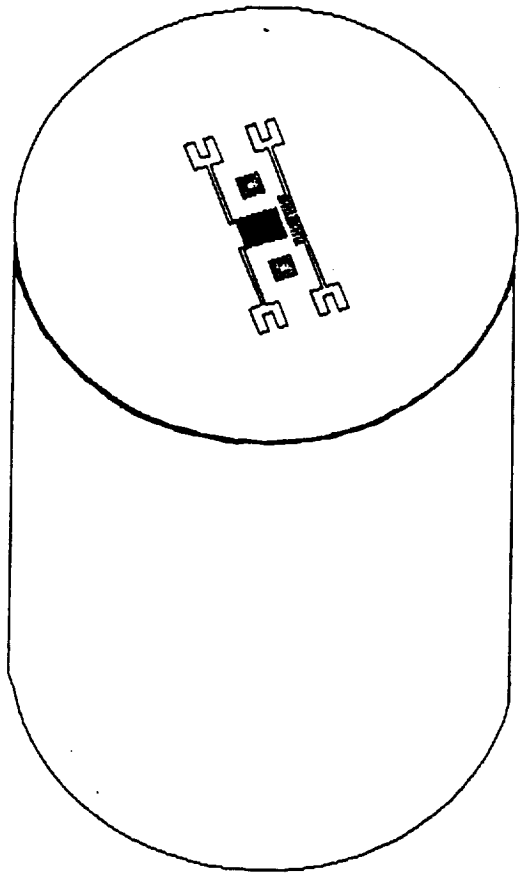

HFM-1
on TPT

Figure 1

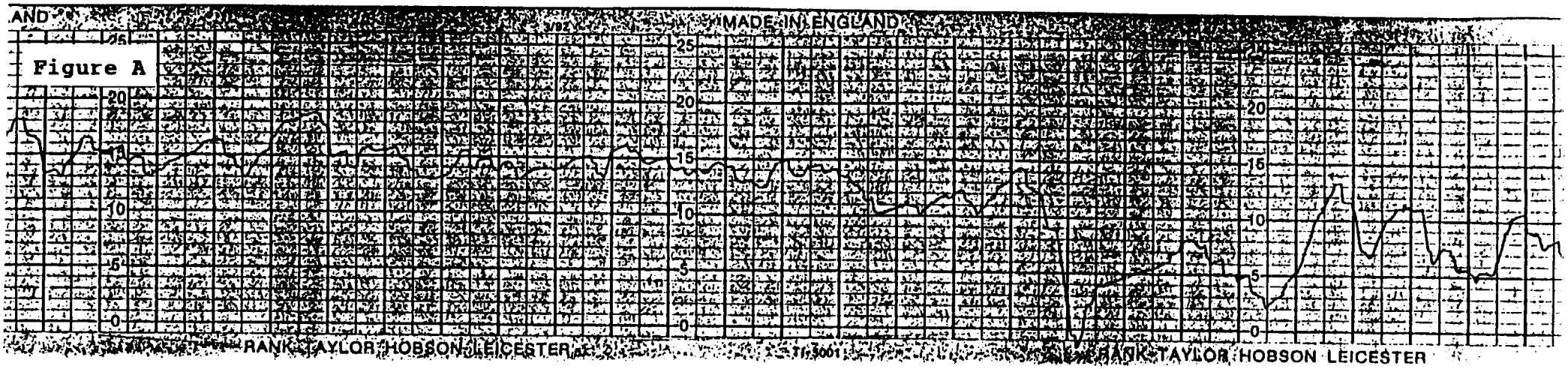

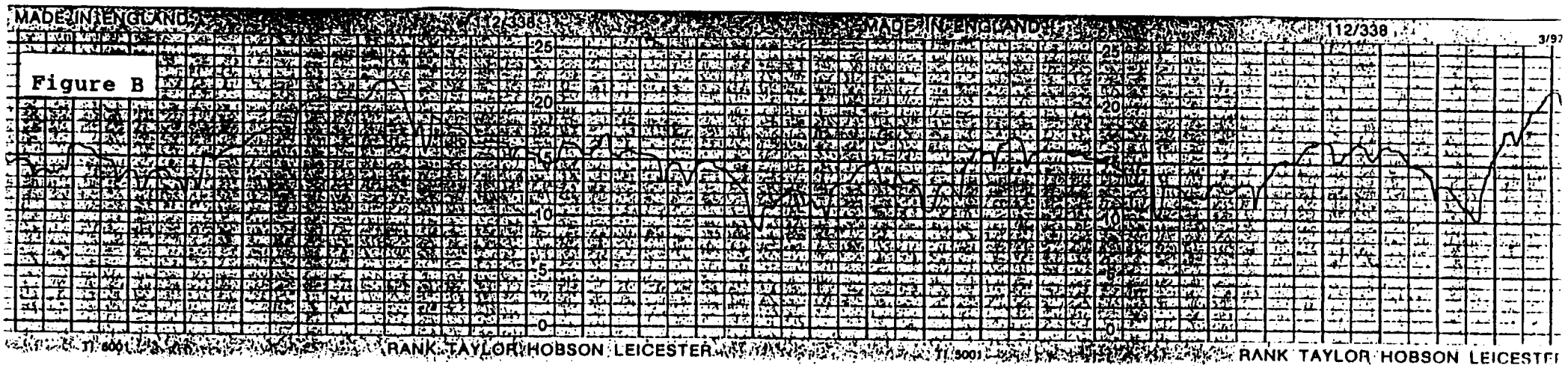

Figure 2

A: TPT Sample #541
Before Polishing
RA ≈ 8.8 - 10 µm

Stylus Profilometer Scan
x scale: 100x
y scale: 500x

B: TPT Sample #3358
Before Polishing
RA ≈ 3 µm

Stylus Profilometer Scan
x scale: 100x
y scale: 2000x

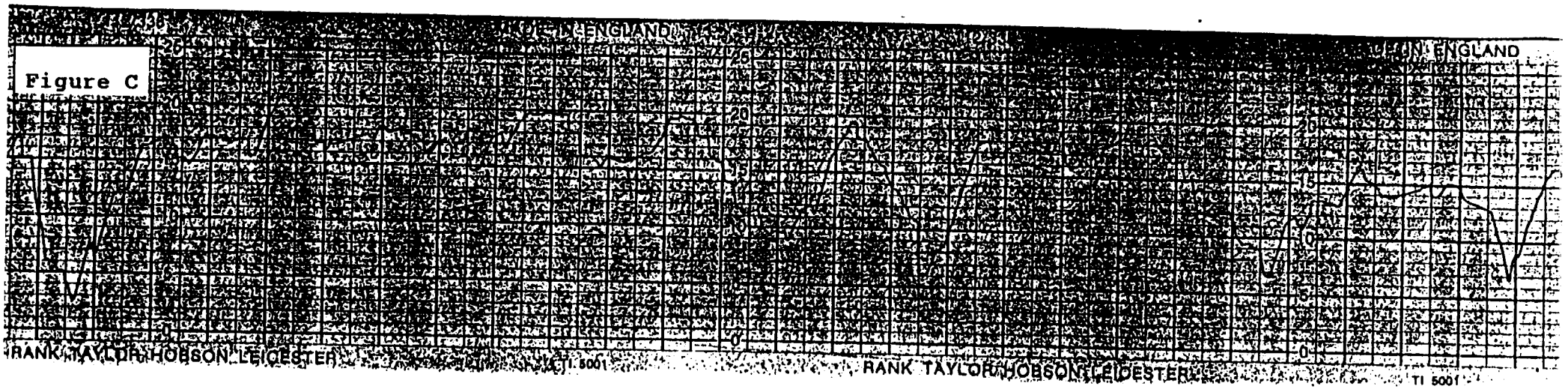

C: TPT Sample #538
Before Polishing
RA ≈ 8.1 - 9.0 µm

Stylus Profilometer Scan
x scale: 100x
y scale: 500x

Figure 2

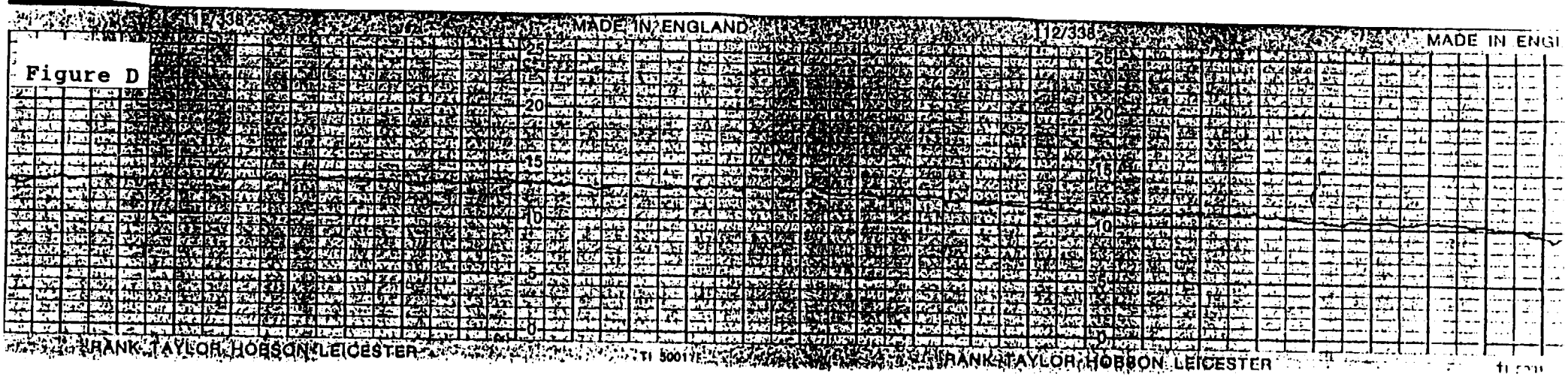

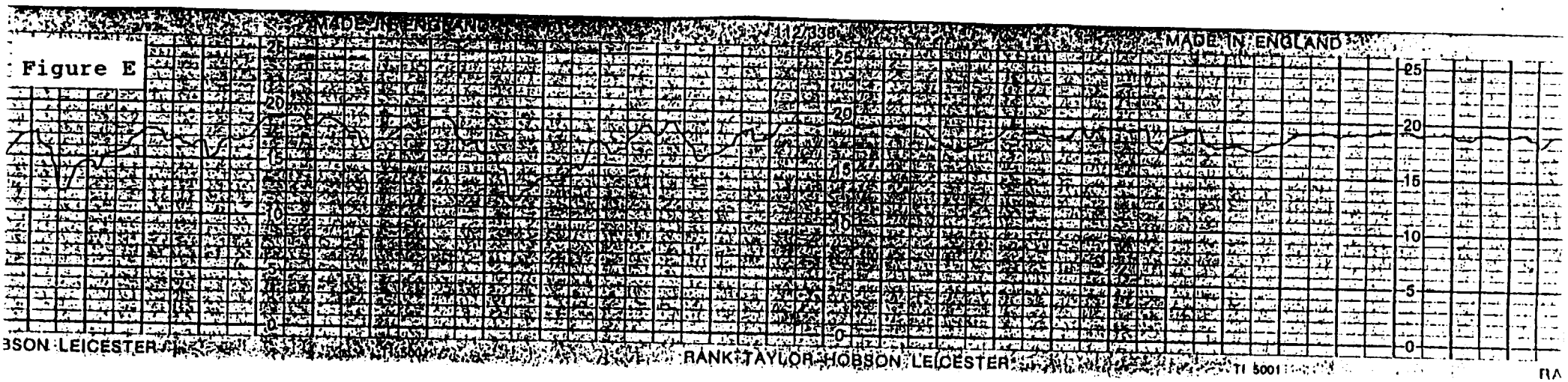

Figure 2

D: TPT Sample #3358
After Polishing
RA ≈ 0.068 - 0.09 µm

Stylus Profilometer Scan
x scale: 100x
y scale: 20,000x

E: TPT Sample #542
After Polishing
RA ≈ 10 µm

Stylus Profilometer Scan
x scale: 100x
y scale: 500x

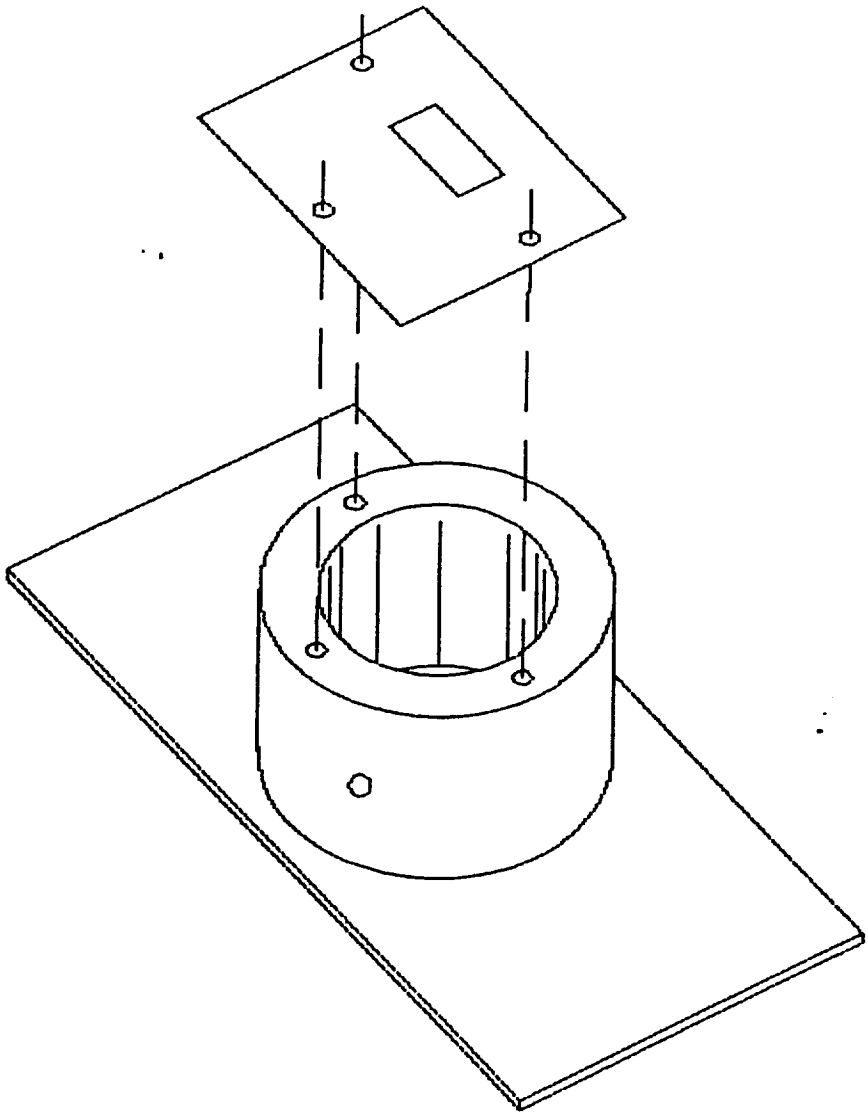

Sputtering Fixture

Figure 3

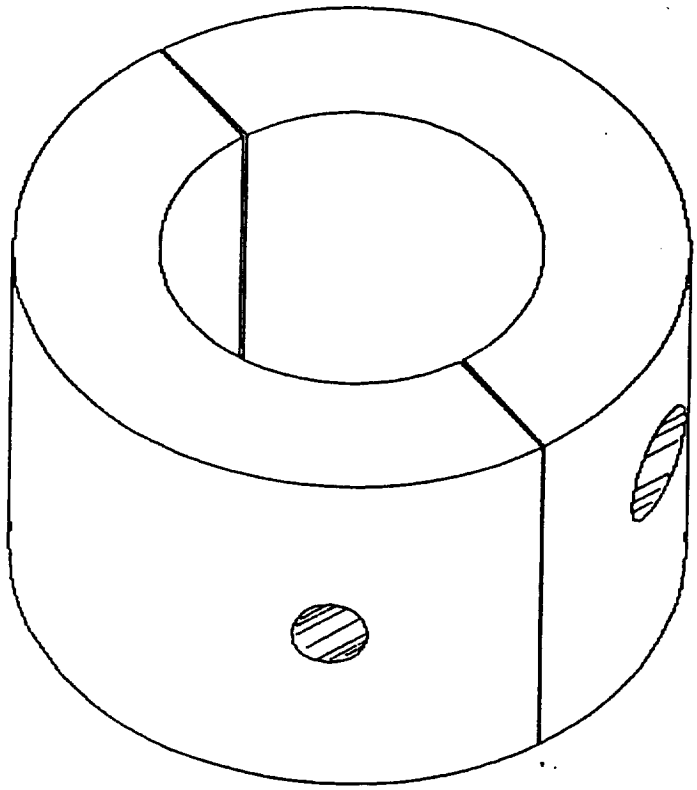

Polishing Fixture

Figure 4

Application of Heat Flux Microsensors to HYFLITE Thermal Protection Tiles

FINAL REPORT - VPI Contract FP-4578-426350

Period of Report - 11/15/93 through 1/14/94

VATELL CORPORATION
P.O. Box 66
Christiansburg, VA 24073

January 17, 1994

SUMMARY

Vatell successfully applied Heat Flux Microsensors to the RCG surfaces of two thermal protection tile core samples, and forwarded the samples to Herb Will of NASA Lewis Research Center for test and evaluation. One of these samples (0077) had connection pads, the other (0078) did not. We recommended that NASA anneal both samples and attempt to apply leads to sample 0077 by parallel gap welding. Success in this would permit the recording of some heat flux data during the initial stage of a destructive test.

During this project we developed methods and process conditions for applying these sensors to thermal protection tiles, and they appear to have achieved good adhesion. The proof of this will be survival of the sensors in arc-jet facility tests by NASA. Because the funding and time allotted to this project were not sufficient for us to explore connection methods for the sensors, the arc-jet tests will not clearly indicate the temperature limits of the sensors without some other form of instrumentation. They should give a general indication of how durable the sensors are, however.

PROCESS DEVELOPMENT

One of the most critical factors in obtaining adhesion of the Heat Flux Microsensor on the RCG coated thermal protection tiles was surface preparation. The preparation required was on both a macro scale and a micro scale.

Macro scale processing required that the surface be ground flat using a 30 micron diamond slurry. The surface was then polished down to 3 micron slurry. It was important throughout the process to handle the sample extremely carefully, to prevent cross contamination, disintegration of the tile and chipping of the RCG coating. The sample polishing process was improved greatly by clamping the tile in a polishing fixture. Cross contamination was reduced by ultrasonically cleaning the sample in its polishing fixture before each reduction in polishing slurry particle size. This method was more effective than the earlier tactic of simply rinsing the surface. The polishing fixture helped to prevent tile disintegration and chipping. We could not completely eliminate chipping, however, because the coated faces of the tile plugs were not perpendicular to the sides. The plugs had to be clamped in the polishing fixture with their faces protruding from the holder. The face of the fixture was not in contact with the polishing surface to completely stabilize the core during the polishing process. The sample was removed from the fixture and subjected to a final ultrasonic cleaning followed by oven drying for 3 - 4 hours. This greatly improved the results.

Micro scale surface preparation consisted of an argon ion shower of the sample face for 60 minutes. Each time a sample was returned to the chamber it was subjected to an additional ion shower to remove contaminants and oxides formed when it was outside the vacuum. Since the HFM is produced by multiple depositions through stainless steel masks, the sample must be removed from the vacuum chamber following each deposition. Previous out-gassing experiments showed that the sample had to be heated for 1.5 to 2 hrs. before ion showering and deposition. Out-gassing was enhanced during ion

showering, especially at elevated temperatures. These surface preparation methods made it unnecessary to deposit a base layer of aluminum oxide.

SENSOR CONSTRUCTION

Two Heat Flux Microsensors were deposited on RCG coated thermal protection tiles, samples 0077 and 0078. Each sample was fabricated using the same methods except for the duration of the pre-cleaning cycle prior to each deposition. A two minute pre-clean was applied to sample 0077 and a four minute treatment was applied to sample 0078 to explore the limit of improvement by ion showering. The longer ion shower removed portions of the metal layers rendering the sensor on sample 0078 inoperable. Film adhesion appeared to be very good, however. Both of the sensors were over-coated with aluminum oxide for physical protection. Since sample 0077 had electrical continuity, extension pads were added, terminating near the edge of the tile, as shown in Figure 1. At the time of deposition it was not known that there would be an attempt to make connections to the sensor by parallel gap welding, so the pads were only deposited to a thickness of 0.3 microns. We did not anneal either sample because we did not have easy access to a vacuum furnace or an annealing furnace with gas purge. From previous experience we know that the platinum-rhodium leads of the sensor will slowly oxidize at the sustained high temperatures of an annealing cycle. The annealing procedure was left for NASA Lewis to perform if necessary.

LEAD ATTACHMENT EXPERIMENTS

After these sensors were completed, we met with NASA personnel to discuss their handling and the future of the project. The project objective is to fabricate thin films on the thermal protection tile surface, ideally in the form of complete sensors, to be tested in the arc jet facility as NASA Ames. Since we were successful in fabricating complete sensors, the discussion concentrated on how to monitor HFM adhesion during the arc jet tests. Without connections being made to the sensors, the point of failure during the tests would be unknown. If there is a way to connect to the sensors, either the voltage signal of the sensor or its resistance could be monitored during a test. This information could then be used in conjunction with a post-test visual inspection to assess damage. The only known method to attach leads to these films is by parallel gap welding. NASA Langley has a parallel gap welder but it is not designed for this type of application. NASA Lewis has the correct equipment and the experience. We decided to deposit simple platinum films to another RCG coated tile sample for lead attachment experiments by NASA Lewis. At this time we learned that the thickness of the thin film at the point of attachment would have to be greater than 2 microns.

We deposited four traces, including two RTS patterns as shown in Figure 2, and then deposited additional material at the edge of the sample to obtain the required thickness for parallel gap welding. This sample was sent to NASA Lewis for lead attachment experiments. They attempted to attach leads to some of the pads by parallel gap welding without success. They decided that annealing would be necessary to achieve a bond.

The sample survived the annealing process and leads were successfully attached. The same method will now be applied to the completed sensors. Since there is increased risk in annealing the multi-layer, composite sensor, the experiments will be performed in stages. Initially the inoperable sensor on sample 0078 will be annealed in a vacuum furnace. The sample will be inspected to establish whether the process was detrimental to the sensor. Additional platinum metal will be deposited on the connection pads of sample 0077 to achieve the required thickness for lead attachment. This will be done by NASA Lewis with stainless steel masks supplied by Vatell. If leads are successfully attached to sample 0078, sample 0077 will then be annealed and have leads attached by the same process.

APPLICATION OF SENSORS TO OTHER MATERIALS

NASA also expressed interest in depositing Heat Flux Microsensors on TUFI coated thermal protection tile samples. Aliza Balter-Peterson forwarded another batch of tile samples to Vatell with several different types of TUFI coatings. The surfaces of these samples were very rough and porous. We attempted to prepare the surfaces for deposition of sensors, using the techniques which had been used on RCG, but without success. The grinding and polishing processes simply exposed more of the same type of surface. Only small unconnected regions of the surface could be polished. It is very unlikely that a sensor would survive on such a surface.

PROPOSED FUTURE EFFORTS

Vatell will supply one additional sensor on an RCG coated thermal protection tile sample by February 1, using the optimum process parameters developed in this contract. The goal is to have a completed Heat Flux Microsensor with leads attached by parallel gap welding, for monitoring of heat flux during the arc jet tests. This is well beyond the original scope of the contract but we believe it is feasible if the tests with samples 0077 and 0078 are successful.

Assuming that the samples provided in this effort survive tests in the arc-jet, the next step in instrumenting thermal protection tiles with Heat Flux Microsensors will be to develop a method for making electrical connections to the sensor leads. Leads attached by parallel gap welding cannot be expected to survive flight conditions long enough to acquire useful data. A number of connection possibilities have been mentioned. One of these is to deposit platinum traces on the inside diameter of a fine silica tube which penetrates the tile surface, and make connections to these traces at the end of the tube on the tile surface. The advantage of this method is that the tube can also be used for static pressure measurements. Methods for applying such tubes to thermal protection tiles have already been developed. Success of this method would require that the gap between the thin film on the surface and the trace in the tube be bridged somehow by sputtered material. This calls for delicate masking procedures, beyond anything we have attempted before. It would also require that the boundary between the outside of the tube and the RCG hold up well enough through the flight to maintain a continuous surface for the thin film

connections crossing it.

A second method for making connections would be to sputter leads around the edge of the thermal protection tile, and make parallel gap welded connections in a more protected area. We are confident that this could be done, but do not know what limitations this would impose on sensor locations or on tile handling and installation. The instrumented tiles would have to have RCG applied around at least one edge and down the side approximately 1/2 inch.

A third method would be to imbed fine (.001-.005") wires in the tile, either directly or in tubes of a material whose thermal expansion coefficient matches that of RCG. The polishing process would expose the ends of these wires, and the sensor pads would be sputtered directly over them. If the wires were fine enough, they might survive the very large temperature gradient at the RCG surface without being isolated by cracks. This technique for making connections to Heat Flux Microsensors has often been discussed but never tried.

While there is reason to be optimistic that one of the above methods will produce reliable connections to Heat Flux Microsensors on thermal protection tiles, further experimentation is required to establish which method is best, and to develop the process itself. In the absence of financial constrainta, all three should be explored. Under the present budgetary conditions, we recommend that only the second and third method be explored. This will take a joint effort of Vatell, NASA Lewis and NASA Ames for approximately a year.

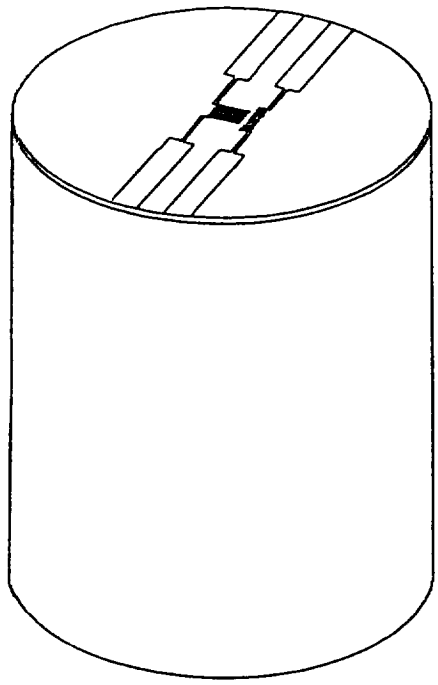

Figure 1 : Heat Flux Microsensor 0077 with extension pads

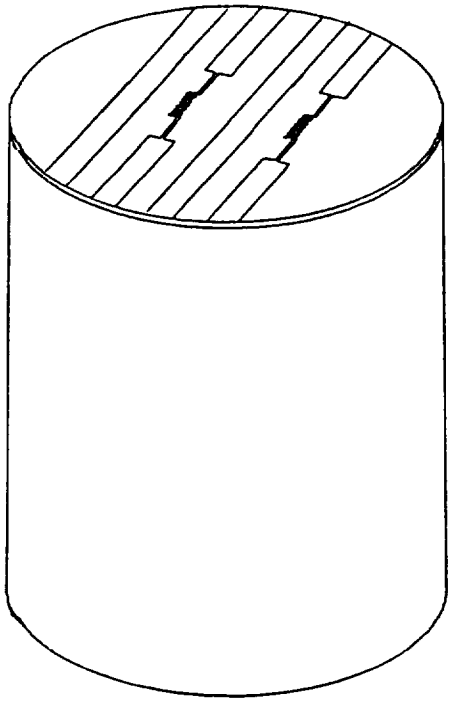

Figure 2 : Four conductors for parallel-gap welding experiments

AIAA

AIAA 94-0730
Shock Tunnel Evaluation of Heat Flux Sensors

D. G. Holmberg
Y. S. Mukkamala
T. E. Diller
Virginia Tech
Blacksburg VA

32nd Aerospace Sciences Meeting & Exhibit
January 10-13, 1994 / Reno, NV

Shock Tunnel Evaluation of Heat Flux Sensors

D. G. Holmberg
Y. S. Mukkamala
Tom Diller*
Mechanical Engineering Department
Virginia Tech
Blacksburg VA 24061-0238

Abstract

A new method is presented for evaluating sensitivity and time response of heat flux gages for use in high speed flows. An advanced transducer, a Heat Flux Microsensor (HFM), is used to produce simultaneous surface heat flux and temperature measurements. It is demonstrated here that a shock tunnel environment can be used for evaluating the performance of these fast-response gages. It is shown how the measurements can be used to check for self-consistency and repeatability of the heat flux calibration.

To verify heat flux sensitivity, simultaneously sampled heat flux and temperature signals are processed using a one-dimensional semi-infinite heat conduction model. Using independently documented thermal properties for the substrate, the heat flux signal can be converted to surface temperature and the temperature signal can be converted to heat flux. Comparing measured and calculated temperatures allows an independent calibration of sensitivity during any short-duration, high-speed flow. The results match gage calibrations performed in convection at the stagnation point of a free jet and done by the manufacturer using radiation.

Time response of the gage can also be estimated in the shock tunnel. The incident shock provides a sharp change in the thermal and flow properties as the shock passes over the wall position of the gage in about 5 μs. The heat flux during this short time is sizable (30 W/cm^2). The microsensor gage recorded a complete heat flux response in less than 10 μs, demonstrating that the Heat Flux Microsensor has a frequency response covering DC to above 100 kHz.

*Professor, Mechanical Engineering, Member AIAA

Nomenclature

C	specific heat, J/kg • K
E_q	Heat flux sensor output, V
E_T	Temperature sensor output, V
h	Gardon gage corrected heat transfer coefficient, W/m^2 • K
k	thermal conductivity, W/m • K
P_o	total pressure, kPa
P_s	surface pressure, kPa
q	heat flux, W/cm^2
q_{act}	measured heat flux, W/cm^2
q_{calc}	heat flux from converted temperature, W/cm^2
S	sensitivity of Heat Flux Microsensor, μV/(W/cm^2)
t	time, s
T_{aw}	adiabatic wall temperature, °C
T_i	reference for temperature sensor, °C
T_o	initial substrate temperature, °C
T_s	surface temperature, °C
T_{act}	measured surface temperature, °C
T_{calc}	surface temperature calculated from heat flux, °C
T_∞	surrounding room temperature, °C
ρ	substrate density kg/m^3
ϵ	emissivity of heat flux gage surface
σ	Boltzmann's constant, W/m^2 • K^4

Introduction

One method of measuring heat flux to or from a surface is to measure the rate of change of temperature of the material. With appropriate transient conduction modeling and material properties, the heat flux that caused the measured temperature history can be determined. The most common method is to assume that the material responds as a one-dimensional, semi-infinite substrate[1-3]. Because this assumption is only valid for sufficiently short times, its use in short-duration flow facilities is natural. The surface temperature measurements are usually made on a low conductivity ceramic substrate. The temperature response is proportional to the square root of the product of thermal conductivity, specific heat, and density of the substrate. Therefore, if a higher conductivity substrate is

used, the temperature response for a given heat flux is smaller.

The use of thin-film resistance gages to measure the required surface temperature history to calculate heat flux has been very successful. Analog electrical circuits are sometimes used for the conversion of the temperature signal to heat flux, but digital data processing or a combination of the two has also been effectively used[4,5]. For use in continuous flow facilities a pre-heated model can be injected into the flow[6]. A group at Calspan has measured heat flux to gas turbine blades[7] using a shock tube to provide the flow conditions for 20 to 25 msec through a gas turbine stage. A group at Oxford University has been instrumental in developing the transient thin-film techniques for many years[8]. Their application has been turbine blades, which were tested in an isentropic light piston tunnel[9]. These are all examples of transient temperature measurements used to determine the time-resolved heat flux.

Roberts et al.[10] used a shock tube to study the transient response of a hot-film sensor. The time required for the incident shock to pass over the gage was estimated as 2 μs for the low pressure ratios used. They measured a fast convection step change due to the shock passage, but also saw some anomalous results. Hayashi et al.[11] measured a large increase in heat transfer resulting from the passage of a shock in Mach 4 supersonic flow. The unsteady heat transfer during the starting transients of a Mach 2.4 flow was measured by Hager et al.[12].

Recently the method of calculating surface temperature from time-resolved heat flux measurements has been demonstrated[13]. This has the advantage that the effects of electrical noise are diminished because the data processing technique is an integration type process. Conversely, the calculation of heat flux from surface temperature is a differentiation type process and tends to greatly increase the apparent electrical noise in the signal. A new thin-film gage which independently measures the surface temperature and heat flux simultaneously was used to demonstrate the correspondence between the heat flux and surface temperature. The heat flux was measured based on the temperature difference across a thin thermal resistance layer deposited on the surface. The combustion events observed had relatively low frequencies (< 100 Hz), however. The match between the heat flux and temperature signals was within the experimental uncertainties of the gage calibrations and material property determinations.

When using heat flux sensors in a high-speed flow, there are two important gage parameters: the gage sensitivity (voltage output/heat flux) and the time response. Neither are easy to measure accurately, particularly in a convective flow environment. A shock tunnel using a supersonic nozzle provides an environment with fast transients, high speed flows, and moderately high heat fluxes. The purpose of this paper is to document a method for using shock tunnel data to determine these gage parameters.

Experimental Facilities and Instrumentation

Shock Tunnel Facility

A schematic of the shock tunnel used for these tests is shown in Fig. 1. The driver section is 8 feet (2.44 m) long, and the driven section 20 feet (6.1 m) long; both the sections are made of three inch inside diameter steel pipes. The driver and driven sections were separated by an aluminum diaphragm holder which housed a mylar diaphragm. A Mach 3 two-dimensional supersonic nozzle is attached to the end of the driven section to obtain supersonic flow, as illustrated in Fig. 2. The nozzle converges from a settling chamber four square inches in cross-section to a throat one square inch in cross-sectional area. It then diverges to the four square inch cross-section exit. A supersonic diffuser with a 10 degree ramp angle is attached to the exit of the nozzle to avoid adverse pressure gradients, and thus boundary layer separation at the exit of the nozzle.

The driver section of the shock tunnel is the high pressure section and is filled with the compressed gas from a bottle. The driven section, for the present research, was left open to the atmosphere. The mylar diaphragm is sized to break at the specified driver gas pressure, which allows the high pressure gas to expand into the low pressure driven section. This sudden expansion produces finite compression waves which eventually coalesce into a traveling shock wave. This incident shock wave travels down the length of the driven section, enters the nozzle, and after the passage of the resultant unsteady waves the nozzle starts. Part of the incident shock is reflected at the nozzle's throat, compressing the gas following it, and creating a stagnant, high pressure, high temperature gas at the nozzle inlet which serves as the gas reservoir for supersonic expansion in the nozzle.

Total and static pressure measurements were made to document the operating characteristics of the

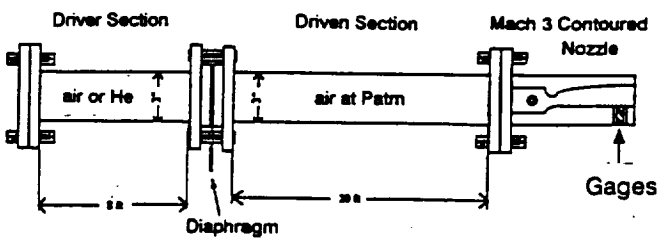

Fig. 1 Shock Tunnel Facility

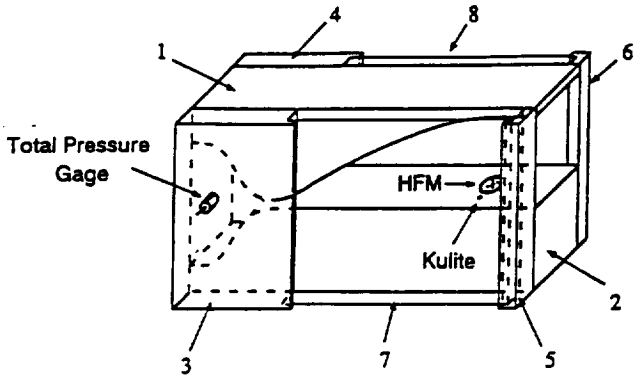

Parts 1&2: Nozzle contour blocks
Parts 3-6: Aluminum side blocks
Parts 7&8: Plexiglass windows

Fig. 2 Shock tunnel nozzle showing gage locations

tunnel. Total pressure measurements were made in the settling chamber upstream of the nozzle throat, while the static pressure measurements were made at the exit of the nozzle at the same axial location as the heat flux measurements (see Fig. 2). The total and static pressure measurements for a run with an air driver at 30.5 kPa (210 psig) and 300 K are given in Fig. 3. The incident shock wave is the initial spike in the pressure trace at 0 ms. The unsteady wave formation and transmission in the nozzle persist until about 5 msec at which time the nozzle starts. The pressure of the heated gas reservoir behind the reflected shock starts dropping after 13 ms, defining the end of the useful run time. The region of low static pressure in the nozzle defines the time of supersonic flow. The nozzle unstarts at 28 msec and the remaining flow is subsonic. Calculations and measurements of the total

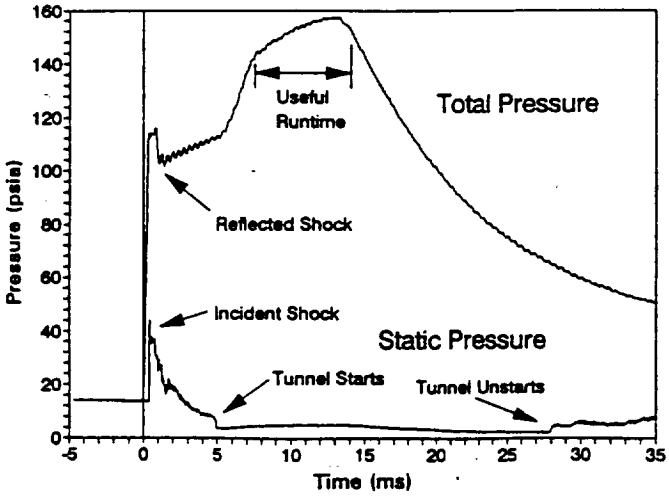

Fig. 3 Total and static pressures for shock tunnel test

temperature in the nozzle indicate an initial total temperature of approximately 600 K. It is this high enthalpy flow that causes the high heat flux and measurable temperature change in the short 40 ms of flow.

To generate a faster shock for time response testing, helium at 29 kPa (200 psig) and 300K was used as the driver gas. For a fixed driver gas to driven gas pressure ratio a lighter driver gas with a larger specific heat yields a faster and stronger incident shock wave. This better approximates an instantaneous step change in heat flux, which is needed for the response time estimation of the heat flux sensor.

Shock Tunnel Instrumentation and Data Acquisition

The heat transfer measurements were carried out with a Heat Flux Microsensor (HFM-3) manufactured by Vatell Corp. This sensor has a flat frequency response to 100 kHz and outputs a voltage directly proportional to the heat flux. A schematic of the sensor is shown in Fig. 4. The heat flux is measured using the output of 280 copper-nickel thermocouple pairs arranged as a differential thermopile. The size of the heat flux sensor on the surface is approximately 4 mm by 6 mm. The calibration

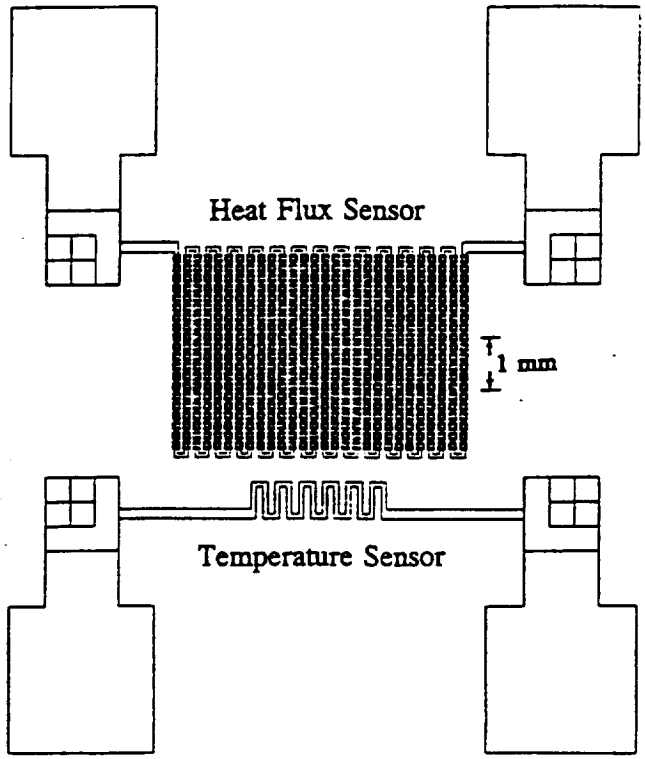

Fig. 4 Detail of HFM overlay pattern

performed by the manufacturer yielded a sensitivity with an uncertainty of ± 10 percent

$$S = \frac{E_q}{q} = 50.0\,\mu V/(W/cm^2) \qquad (1)$$

where E_q equals the output voltage from the sensor and q the heat flux. An independent convection calibration (described below) produced a sensitivity of 49.2 ± 5 percent, and is in excellent agreement.

In addition, the HFM has a nickel resistance element which provides an independent measure of the surface temperature. A 0.1 mA current is supplied to the sensor through an amplifier unit supplied with the gage to provide the resistance measurement. The manufacturer's calibration to convert the voltage signal to surface temperature T_s is

$$T_s - T_i = (28055\,°C/V)\,E_T \qquad (2)$$

where E_T is the unamplified voltage, and T_i is an initial reference temperature.

The sensors were fabricated on a 2.5 cm diameter aluminum nitride substrate by a sputtering process. The thermal properties of the substrate ($k = 165$ W/m•K, $C = 713$ J/kg•K, $\rho = 3290$ kg/m^3, $\sqrt{k\rho c}$ uncertainty ± 5%) are close to those of the aluminum nozzle where the gage is mounted. Four pins were countersunk into the substrate to bring the surface temperature and heat flux signals from the surface to the tunnel exterior without disturbing the flow. The HFM was mounted flush with the bottom surface of the shock tunnel, near the exit plane of the nozzle, as illustrated in Fig. 2. Silicone sealant was used to prevent air injection around substrate during runs.

Two pressure measurements were taken. Static pressure was measured with a Kulite type XCQ-062 miniature pressure transducer. Total pressure in the settling chamber upstream of the nozzle was measured using a Lucas-Shaevitz total pressure transducer. Both of these pressure signals were amplified using a Measurements Group, Inc. 2310 signal conditioning amplifiers, with a 1 kHz low pass filter used on the total pressure signal to suppress a 4 kHz ringing present in the settling chamber during tunnel start-up.

For the purpose of gage sensitivity analysis, two channels of data were sampled using an HP 3562A Dynamic Signal Analyzer. A sampling rate of 50 kHz was used in recording 40 ms traces of the pressure signals. Heat flux and temperature signals from the HFM were sampled at 25 kHz for 80 ms.

For time response analysis, a LeCroy 6810 Waveform Digitizer was used to sample the HFM at a 1 μs interval. The faster sample rate allowed better resolution of the incident shock.

Convection Calibration

Convection calibration of the heat flux sensor was performed by the apparatus shown in Fig. 5. The HFM is placed in the stagnation region of an air jet. An air jet is produced by a high pressure blower that pumps air into a plenum and through an orifice (3.8 cm diameter) in the end plate. The heat flux gage is placed perpendicular to this jet at a distance of three orifice diameters (11.4 cm). The heat flux gage is held in an aluminum cylinder which in turn is inserted through a hole in a steel plate so that gage, cylinder and plate are together flush and perpendicular to the impinging jet. The aluminum cylinder is wrapped with a resistance heater pad which provides heat to the gage. From earlier tests with a reference Gardon gage, a heat transfer coefficient of $h = 213$ W/m^2•K was found for this particular configuration. The Gardon gage results were corrected as specified for convection by Borell and Diller[14].

Before calibration was performed, the adiabatic wall temperature was determined by operating the air jet with the heater turned off. The steady-state surface temperature of the gage was assumed to be equal to the adiabatic wall temperature, T_{aw}. The value was approximately 1 °C below the temperature of the air in the plenum. For the calibration the heater was activated and system was allowed to reach thermal equilibrium. The surface temperature and heat flux output voltage, E_q, were recorded. The heat flux was then calculated according to

$$q = h_c (T_s - T_{aw}) + \sigma\epsilon (T_s^4 - T_\infty^4) \qquad (3)$$

where ϵ is the estimated gage emissivity; the right-hand part of the expression is a small radiation correction. Using this heat flux q and the heat flux output voltage, E_q, the gage sensitivity was found

$$S = \frac{E_q}{q} \qquad (4)$$

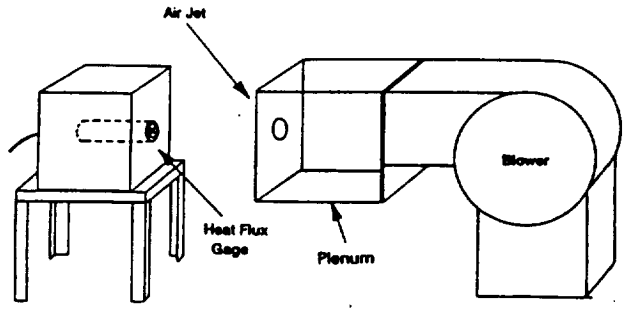

Fig. 5 Convection calibration apparatus

Different power levels were used to complete the calibration process.

Data Conversion, Digital Data Processing Routine

To convert measured heat flux and surface temperature to the corresponding calculated values a one-dimensional, semi-infinite model of the heat transfer in the substrate was used. The substrate was assumed to initially be at a uniform temperature, T_o. Cook and Felderman[15] developed a numerical approximation for heat flux from discrete temperature steps using a piecewise linear model of the temperature trace

$$q(t_n) = \frac{2\sqrt{k\rho C}}{\sqrt{\pi}} \sum_{j=1}^{n} \frac{T_j - T_{j-1}}{\sqrt{t_n - t_j} + \sqrt{t_n - t_{j-1}}} \qquad (5)$$

This is ideal for processing digital data. In similar fashion Baker and Diller[13] developed a method for calculating the time-resolved surface temperature from the measured heat flux signal. Using a Green's function approach individual heat flux impulse solutions were combined to include a series of heat flux data points.

$$T_s(t_n) - T_o = \frac{2}{\sqrt{\pi}\sqrt{k\rho C}} \sum_{j=0}^{n-1} q_j \left[\sqrt{t_n - t_j} - \sqrt{t_n - t_{j+1}} \right] \qquad (6)$$

A computer code was written making use of these equations to process E_q and E_T. In addition, the code calculates the gage sensitivity by minimizing the sum of the errors between individual time values of T_{act} and T_{calc}. By this method, an independent measure of gage sensitivity can be obtained for each data sample (one test run of the shock tunnel).

Results

Gage Sensitivity Calibration

Using temperature and heat flux signals from the Heat Flux Microsensor (HFM) processed according to the digital-data-processing routine presented above, an independent measure of gage sensitivity, S, can be found. This measure of S has particular value because it is determined in the actual high speed flow and high temperature environment of the test.

As an example of the method, the heat flux and temperature signals for one test are presented in Fig. 6. Notice the two initial peaks in the heat flux. These are due to the incident and reflected shock waves. The tunnel starts at 5 ms, and unstarts at 28 ms (refer back to Fig. 3 for the corresponding pressure traces). Notice also that heat flux becomes negative at about 45 ms as the temperature of the flow drops, and the stored energy in the gage substrate goes back into the flow.

These HFM temperature and heat flux signals were converted to the corresponding heat flux and surface temperature values using equations (5) and (6). Comparison of the actual gage surface temperature (T_{act}) with the calculated gage surface temperature (T_{calc}) is shown in Fig. 7. There is excellent agreement between T_{act} and T_{calc}, demonstrating the accuracy of the one-dimensional model. Although it is difficult to separate the two curves because of their overlap, the curve calculated from the heat flux is much smoother than the measured temperature curve because of the integration process represented by equation (5).

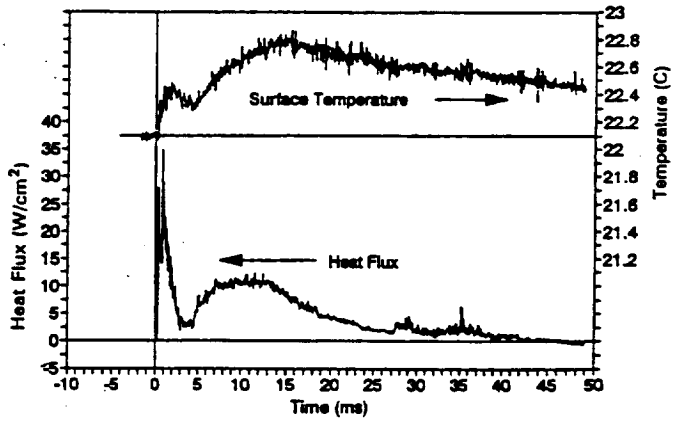

Fig. 6 Surface temperature and heat flux for shock tunnel test

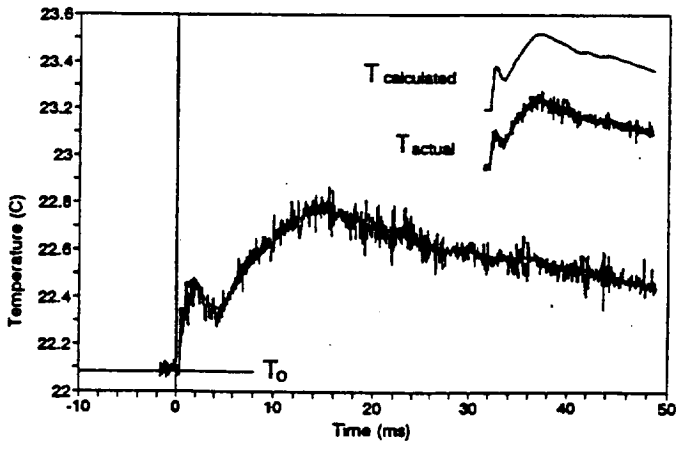

Fig. 7 Actual temperature and temperature calculated from heat flux

To quantify the fit between the two curves, the data conversion program was used to calculate the needed value of the heat flux sensitivity, S, to minimize the error between T_{act} and T_{calc}. For the data over the entire 80 ms of the test, the program yielded S = 43.5 μV/(W/cm^2), which was used to calculate the surface temperature and heat flux curves in Figs 7 and 8. For shorter data sets near the start of the run (e.g. the first 20 ms), higher optimal sensitivities were found. If only the incident shock is examined, an optimized sensitivity of S = 49.1 μV/(W/cm^2) results. This is in excellent agreement with the manufacturer supplied calibration of S = 50.0 μV/(W/cm^2) and the value obtained in convection calibration of S = 49.2 (μV/W/cm^2). A second test run produced similar results, with optimized sensitivities showing the same trend, but with values approximately 4% higher, and thus in better agreement with the sensitivities determined by other means. Most of these values of S are within the experimental uncertainties of the sensitivities determined by convection and radiation.

Comparison of the actual heat flux (q_{act}) with the calculated heat flux (q_{calc}) can also be used to determine S, but q_{calc} is an extremely noisy curve as shown in Fig. 8. Because heat flux is proportional to the time rate of change of temperature, the effects of electrical noise are increased when converting from temperature to heat flux because the data processing is a differentiation type process. It should be noted that the standard method is to obtain heat flux from the surface temperature, while the current work converts from heat flux to temperature, which gives much better signals. Nonetheless, the agreement in the mean q_{calc} with the less noisy q_{act} confirms the accuracy of S.

It should be noted that the accuracy of the data conversion routine is limited to short run-times only

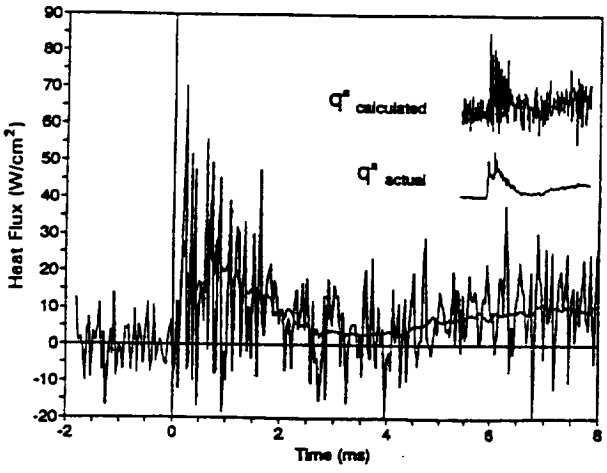

Fig. 8 Actual heat flux and heat flux calculated from temperature

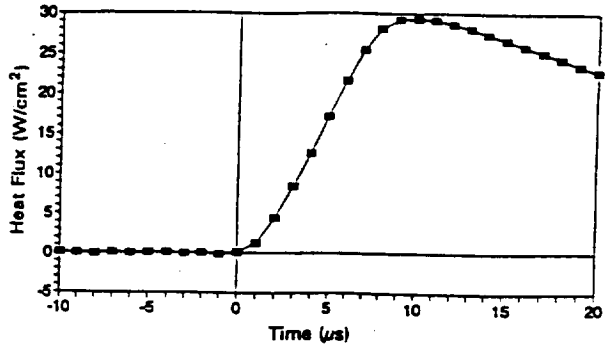

Fig. 9 Heat flux response to incident shock

(<0.15 sec for this substrate), due to the semi-infinite conduction assumption[13]. But it is also important to note that even though the data analysis for calculating surface temperature is limited to short run times, the calibratedsensitivity and the temperature and heat flux measured by the microsensor are valid for any length of time.

Time Response Tests

In previous work a Bragg cell and laser were used to estimate the time response of the heat flux gage[16]. Unfortunately, the laser irradiation required an absorption coating which severely altered the response time. Because the shock tunnel is based on convection heat transfer, this problem is eliminated. The incident shock provides a sharp change in the thermal and flow properties as the shock passes over the wall position of the gage in about 5 μs. Fig. 9 shows an expansion of the spike corresponding to the incident shock passage in Figs. 3 and 6. The scale has been expanded from milliseconds to microseconds and the individual data points are marked for the 1 MHz sampling rate. No filtering was used for this data. The heat flux during this short time is sizable (30 W/cm^2). The microsensor gage recorded a complete heat flux response in less than 10 μs. Therefore, the gage has been shown to cover a bandwidth from dc to at least 100 kHz.

Conclusions

A method has been developed for determining heat flux gage sensitivity for the Heat Flux Microsensor (HFM) from shock tunnel test data. Using a simple data processing code, measured heat flux can be converted to surface temperature and compared with the measured temperatures. By minimizing the difference between these two data sets, an independent measure of sensitivity can be determined for each test run. These values can then be compared with sensitivity calibrations performed by other means and as a check for changes in sensitivity while testing is being performed.

A shock tunnel has also been used to measure the time-response of the HFM. The incident shock in a shock tunnel test produces the equivalent of a step-rise in heat flux in a convection environment. The gage's performance in responding to this step change gives a measure of time response. The gage used in these tests has been shown to cover a bandwidth from DC to 100 kHz.

Because the high speed and high temperature flow in a shock tunnel is similar to the environment often encountered in heat flux testing, the sensitivities and time response determined in the shock tunnel are particularly appropriate.

Acknowledgments

The authors gratefully acknowledge support for this research from the U. S. Air Force Office of Scientific Research under the supervision of Major Dan Fant, program manager.

References

[1]Scott, C. J., "Transient Experimental Techniques for Surface Heat Flux Rates," in **Measurements in Heat Transfer**, Eds. E. R. G. Eckert and R. J. Goldstein, McGraw-Hill, New York, 1976, pp. 375-396.

[2]Jones, T. V., "Heat Transfer, Skin Friction, Total Temperature, and Concentration Measurements," in **Measurements of Unsteady Fluid Dynamic Phenomena**, Ed. B. E. Richards, Hemisphere Pub. Co., Washington DC, 1977, pp. 63-102.

[3]Diller, T. E., "Advances in Heat Flux Measurements," **Advances in Heat Transfer**, Vol. 23, Eds. J. P. Hartnett et al., Academic Press, Cambridge, 1993, pp. 279-368.

[4]George, W. K., Rae, W. J., Seymour, P. J., and Sonnenmeier, J. R., "An Evaluation of Analog and Numerical Techniques for Unsteady Heat Transfer Measurement with Thin Film Gauges in Transient Facilities," **Experimental Thermal and Fluid Science**, Vol. 4, 1991, pp. 333-342.

[5]Dunn, M. G., George, W. K., Rae, W. J., Woodward, S. H., Moller, J. C., and Seymour, P. J., "Heat-Flux Measurements for a Full-Stage Turbine: Part II – Description of Analysis technique and Typical Time-Resolved Measurements, **ASME Journal of Turbomachinery**, Vol. 108, 1986, pp. 98-107.

[6]O'Brien, J. E., "A Technique for Measurement of Instantaneous Heat Transfer in Steady-Flow Ambient-Temperature Facilities," **Experimental Thermal and Fluid Science**, Vol. 3, 1990, pp. 416-430.

[7]Dunn, M. G., "Phase and Time-Resolved Measurements of Unsteady Heat Transfer and Pressure in a Full-Stage Rotating Turbine," **ASME Journal of Turbomachinery**, Vol. 112, 1990, pp. 531-538.

[8]Schultz, D., and Jones, T. V., "Heat Transfer Measurements in Short Duration Hypersonic Facilities," AGARDograph 165, 1973.

[9]Nicholson, J. H., Forest, A. E., Oldfield, M. L. G., and Schultz, D. L., "Heat Transfer Optimized Turbine Rotor Blades--An Experimental Study Using Transient Techniques," **ASME J. Eng. for Gas Turbines and Power**, Vol. 106, 1987, pp. 173-182.

[10]Roberts, A. S., Jr., Ortgies, K. R., Gartenberg, E., and Caraway, D. L., "Convective Response of a Wall-Mounted Hot-Film Sensor in a Shock Tube," in International Symposium on Nonsteady Fluid Dynamics, Eds. J. A. Miller and D. P. Telionis, ASME, N.Y., 1990, pp. 253-258.

[11]Hayashi, H., Aso, S., and Tan, A., "Fluctuation of Heat Transfer in Shock Wave/Turbulent Boundary-Layer Interaction," **AIAA Journal**, Vol. 27, 1989, pp. 399-404.

[12]Hager, J. M., Onishi, S., Langley, L. W., and Diller, T. E., "High Temperature Heat Flux Measurements," **AIAA Journal of Thermophysics**, Vol. 7, 1993, pp. 531-534.

[13]Baker, K. I., and Diller, T. E., "Unsteady Surface Heat Flux and Temperature Measurements," ASME Paper No. 93-HT-33, 1993.

[14]Borell, G. J., and Diller, T. E., "A Convection Calibration Method for Local Heat Flux Gages," **ASME Journal of Heat Transfer**, Vol. 109, 1987, pp. 83-89.

[15]Cook, W. J., and Felderman, E. M., "Reduction of Data From Thin Film Heat-Transfer Gages: A Concise Numerical Technique," **AIAA J.**, Vol. 4, 1966, pp. 561-562.

[16]Hager, J. M., Simmons, S., Smith, D., Onishi, S., Langley, L. W., and Diller, T. E., "Experimental Performance of a Heat Flux Microsensor," **ASME Journal of Engineering for Gas Turbines and Power**, Vol. 113, 1991, pp. 246-250.